J. King Saud Univ., Vol. 1, *Eng. Sci.* (1,2), pp. 147-160, Riyadh (1409/1989)

Cross-Polarized Current Analysis and Control for Parabolic Reflector Antennas

Mostafa S. Afifi
Electrical Engineering Department, College of Engineering, King Saud University, P.O. Box 800, Riyadh 11421, Saudi Arabia

Abstract. Analyses are presented for the current distribution and its effects on the radiated fields from any portion of the parabolic reflector, using a generalized feed source. The feed is formed of co-polarized electric and magnetic sources, with a given directivity towards the reflector surface. The mixture ratio between the electric and magnetic sources is examined with a view to minimize the cross-polarized radiation. This ratio is dependent on the reflector configuration. While it is well known that cross-polarized currents vanish when the electric and magnetic moments of the feed are equal in symmetric reflectors, no comprehensive analyses are available for offset configurations. Therefore, in this work generalized rigorous analyses are given to specially accommodate offset reflectors, which are widely used in modern telecommunication systems.

Cross-polarized currents of offset reflectors could only be minimized. Feed pointing would be lower than the reflector center (mid way between this center and the vertex). Also, the feed source should be predominantly electric for vertical polarization and predominantly magnetic for horizontal polarization. Illustrations based on computer simulation are presented to give quantitative perspective for these results.

1. Introduction

Definitions of the cross-polarized radiation of generalized electric and magnetic source radiators are given in the reference [1]. This was followed by derivation of general expressions for the currents induced on the surface of an axially symmetric parabolic reflector, center fed by arbitrary combination of radiating sources [2]. In the optimum situation, when the electric and magnetic sources are of equal moments (the situation known in the literature by "Huygens source" [3]), the radiation of the cross-polarized fields from the reflector are generated only by its surface curvature, which was proved to be of second order of importance [2,4]. The blockage caused by the feed and its supporting structure, however, destroys this advantage, yielding high radiation levels of scattered main and cross-polarized lobes. For this reason modern systems employ offset parabolic reflectors in order to avoid these blockage effects. Therefore, this paper handles the cross-polarized currents and fields of the reflector in a general form, with emphasis on the offset parabola.

Definitions are first established for the used electromagnetics, with electric and magnetic feed sources. Then the frequency reuse capability of offset reflectors, employing dual orthogonally polarized signals, is discussed using a general derivation for the induced currents on the reflector surface from an appropriate feed composed of specific mixture of electric and magnetic source radiators. Specific offset parabolic reflector designs [3,5] are used here as design tests for the derived results.

2. Hertz Electric and Magnetic Vector Potentials

The uncurl of Maxwell's equation, of the form

$$\nabla \times \bar{E}_e = - \frac{\partial \bar{B}}{\partial t} = - \frac{\partial \nabla \times t \bar{A}}{\partial t}$$

yields the radiated electric field due to electric sources, as function of the magnetic vector potential A and the electric scalar potential V, which is given by:

$$\bar{E}_e = - \frac{\partial \bar{A}}{\partial t} - \nabla V \tag{1}$$

In general the Hertz electric vector potential $\bar{\Pi}$ can only be used to derive this electric field vector, instead of using both the magnetic vector potential $\bar{A}$ and the electric scalar potential V, of equation (1). The magnetic vector potential $\bar{A}$ and the scaler potential V are related to the Hertz electric vector potential $\bar{\Pi}$ through the relations [6]

$$\bar{A} = \mu \varepsilon \frac{\partial \bar{\Pi}}{\partial t} \quad \text{and} \quad V = - \nabla . \bar{\Pi} \tag{2}$$

where μ and ε are respectively the permeability and the permitivity of the medium. Using well known vector analysis manipulations with $\bar{A}$ and V yields

$$\bar{E}_e = \nabla \times \nabla \times \bar{\Pi}.$$

Also, similar uncurling of the other Maxwell's equation yields the radiated magnetic field vector $\bar{H}_e$ (generated from the electric current sources) and given by:

$$\bar{H}_e = \varepsilon \frac{\partial}{\partial t} \nabla \times \bar{\Pi}.$$

It is also possible to show that the Hertz magnetic vector potential $\bar{\Pi}^*$ exists, with similar relations for the electric vector and the magnetic scalar potentials given by

$$\bar{A}^* = \mu \varepsilon \frac{\partial \bar{\Pi}^*}{\partial t} \quad \text{and} \quad V_m = - \nabla . \bar{\Pi}^* \tag{3}$$

These are used in a similar procedure as the previous section yielding

$$\bar{H}_m = \nabla \times \nabla \times \bar{\Pi}^*$$

and

$$\bar{E}_m = -\mu \frac{\partial}{\partial t} \nabla \times \bar{\Pi}^*$$

2.1. Combined Fields of Both Potentials

The total electric and total magnetic fields due to both Hertz electric and magnetic potentials, and as also derived by Stratton [6], are then given by

$$\bar{E}_t = \nabla \times \nabla \times \bar{\Pi} - \mu \frac{\partial}{\partial t} \nabla \times \bar{\Pi}^* \tag{4}$$

and

$$\bar{H}_t = \nabla \times \nabla \times \bar{\Pi}^* + \varepsilon \frac{\partial}{\partial t} \nabla \times \bar{\Pi} \tag{5}$$

hese relations are exact in representing the radiated electric and magnetic fields from knowledge of both Hertz (electric and magnetic) sources of radiation, without using the four (scalar electric, scalar magnetic, electric vector and magnetic vector) potentials. In the far field, however, the effects of the scalar potentials diminish, reducing the latter four potentials to only two, and yielding

$$\bar{E}_e = -\frac{\partial \bar{A}}{\partial t} \quad \text{and} \quad \bar{H}_m = -\frac{\partial \bar{A}^*}{\partial t} \tag{6}$$

These relations appear to be simple. They imply, however, difficulties in relating the magnetic vector potential to electric sources and relating the electric vector potential to magnetic sources. Also $\bar{A}$ and $\bar{A}^*$ need to be projected along $\bar{E}_e$ and $\bar{H}_m$ in the far field, and followed by computations of $\bar{H}_e$ from $\bar{H}_e$ and $\bar{E}_m$ from $\bar{H}_m$, with final fields given by

$$\bar{E}_t = \bar{E}_e + \bar{E}_m \quad \text{and} \quad \bar{H}_t = \bar{H}_e + \bar{H}_m \tag{7}$$

This shows that the use of Hertz vector potentials is simple. It is as simple as that $\bar{\Pi}$ is parallel to the source electric field and $\bar{\Pi}^*$ is parallel to the source magnetic field. Moreover, it is exact in the near and in the far fields. This fact is absent from the literature. The discussion of this section fills in this gap and clarifies the procedure used in this paper.

3. Reflector Configuration

The reflector configuration is chosen so that the focal point is at the origin of the three dimensional coordinate system, with the main axis of the reflector along the Z-axis. The reflector vertex (or the virtual vertex in case of full offset) is on the negative Z-axis at a distance equal to the focal length "F" from the origin. An illustration of this configuration is shown in Fig. 1. In this figure $\hat{a}_n$ is the unit vector normal to the surface of the parabolic reflector, given by

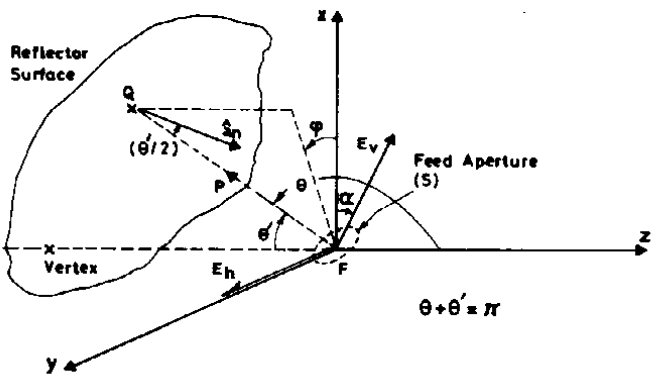

Fig. 1. The reflector Configuration

$$\hat{a}_n = -\cos(\theta/2)\cos\varphi\,\hat{a}_x - \cos(\theta/2)\sin\varphi\,\hat{a}_y + \sin(\theta/2)\,\hat{a}_z,$$

p is the distance from the focal point to a point Q on the reflector surface and $\hat{a}_p$ is the unit vector along p given by

$$\hat{a}_p = \sin\theta\cos\varphi\,\hat{a}_x + \sin\theta\sin\varphi\,\hat{a}_y + \cos\theta\,\hat{a}_z.$$

For a given feed aperture, at the focal point, the source radiators are assumed to be parallel arrays of electric fields and magnetic fields. Both sources are assumed orthogonal, which is a requirement for purity of polarization. Also the feed radiating aperture has tilt angle α from the vertical, so that its peak radiation is directed to the central areas of the offset configurations.

The Hertz electric vector potential $\bar{\Pi}$ is parallel to the electric field polarization vector, having a direction given by $\hat{a}_e$, with magnitude proportional to the orthogonal magnetic field strength H (which is the effective electric current source). Using harmonic time function given by exp (jωt) the first part of equation (2) yields.

$$\bar{\Pi} = \frac{1}{j\omega\,\varepsilon}\int_s \frac{(H)}{4\pi P}\, e^{-j\beta p}\; ds\,\hat{a}_e = \frac{f(\theta,\varphi)}{\varepsilon}\, a_e \frac{e^{-j\beta p}}{P}\,\hat{a}_e,$$

where S is the surface area of the source aperture and H is tangential to this aperture, a_e is the amplitude of the source magnetic field, relative to Huygens source plane wave radiator, ω is the radial frequency, ß is the phase constant and $f(\theta,\varphi)$ is a directivity function determined by this primary source radiation pattern.

Similarly, the orthogonal Hertz magnetic vector potential $\bar{\Pi}^*$ is parallel to the direction $\hat{a}_m$ has a magnitude proportional to the electric field strength E (which is the effective magnetic current source) and is derivable using the first part of equation (3), yielding

$$\bar{\Pi}^* = \frac{1}{j\omega\sqrt{\mu\,\varepsilon}}\int_s \frac{(E)\, e^{-j\beta P}}{4\pi P}\; ds\,\hat{a}_m = \frac{f(\theta,\varphi)}{\sqrt{\mu\varepsilon}}\; a_m \frac{e^{-j\beta P}\,\hat{a}^{m}}{P},$$

where a_m is the amplitude of the source electric field relative to Huygens source of plane waves. The directivity $f(\theta,\varphi)$ is assumed the same, for similar distribution of electric and magnetic sources, which closely approximates practical situations. Substitution of these relations in equations (4) and (5), and using the far field relations

$$\nabla \times \nabla \times \bar{\Pi} = -\,\beta^2\;\hat{a}_P \times \hat{a}_P \times \bar{\Pi}$$

and

$$\nabla \times \bar{\Pi} = -\,j\beta\hat{a}_P \times \bar{\Pi}$$

yield the feed radiated fields at point Q, given by

$$\bar{E}_t = -\,\beta\omega Z\left\{a_e(\hat{a}_P \times \hat{a}_P \times \hat{a}_e) + a_m(\hat{a}_P \times \hat{a}_m)\right\} \qquad f(\theta,\varphi)\,\frac{e^{-j\beta P}}{P} \qquad (8)$$

and

$$\bar{H}_t = -\,\beta\omega\left\{a_m \times \hat{a}_P \times \hat{a}_P \times \hat{a}_m) - a_e(\hat{a}_P \times \hat{a}_e)\right\} \qquad f(\theta,\varphi)\,\frac{e^{-j\beta p}}{P} \qquad (9)$$

where Z is the free space intrinsic impedance (377 Ohms)

4. Surface Current Distribution

The feed radiated magnetic field $\bar{H}_t$ is usable to derive the current density distribution on the reflector surface, using the well known physical optics relation [3,7]

$$\bar{K}_s = 2(\hat{a}_n \times \bar{H}_t) \qquad (10)$$

which proved to be adequate for computations of the reflector radiated fields [3,4,7] with negligible errors. The radiated polarization is determined by the polarity of these currents, *i.e.* if the polarization is vertical, the vertically projected currents form the main sources of polarization. The horizontally projected currents form mainly then the cross polarized radiation. This statement is derivable directly from equations (6) and (7), where the polarities of $\bar{E}$ and $\bar{H}$ are mainly the polarities of the electric and magnetic currents, which are the sources of the magnetic vector and the electric vector potentials, respectively.

In the following investigations different source requirements are obtained which would minimize the cross polarized currents. The radiation conditions which determine the levels and width of the cross-polarized main lobes, relative to the main beam level, are derived in simple terms in order to illustrate the resulting radiation levels of the source currents.

4.1. Vertically Polarized Sources

Vertically polarized sources (as shown in Fig. 1) have the electric unit vector of polarization given by

$$\hat{a}_{ev} = \cos\alpha\,\hat{a}_x + \sin\alpha\,\hat{a}_z$$

and the magnetic unit vector of polarization given by

$$\hat{a}_{mv} = -\hat{a}_y .$$

Substitution of these into equation (9), for the radiated magnetic field, yields

$$\bar{H}_{tv} = -2\omega\beta\, f(\theta,\varphi)\left\{\hat{a}_x H_x + \hat{a}_y H_y + \hat{a}_y H_z\right\}\frac{e^{-j\beta\rho}}{\rho} \tag{11}$$

where

$$H_x = -a_m \sin^2\theta \sin\varphi\cos\varphi - a_e \sin\alpha \sin\theta \sin\varphi,$$

$$H_y = a_m(\cos^2\theta + \sin^2\theta\cos^2\varphi) - a_e(\cos\alpha\cos\theta - \sin\alpha\sin\theta\cos\varphi),$$

and

$$H_z = -a_m \sin\theta\cos\theta\sin\varphi + a_e \sin\theta\sin\varphi\cos\alpha.$$

Substitution in equation (10) yields the current density distribution on the reflector surface given by

$$\bar{K}_v = -2\omega\beta\, f(\theta,\varphi)\left\{ -\hat{a}_x [H_z \cos(\theta/2)\sin\varphi + H_y \sin(\theta/2)] + \hat{a}_y [H_x \sin(\theta/2) + H_z \cos(\theta/2)\cos\varphi] + \hat{a}_z [H_x \cos(\theta/2)\sin\varphi - H_y \cos(\theta/2)\cos\varphi] \right\} \frac{e^{-j\beta p}}{P} \qquad (12)$$

This current density is polarized predominantly along the x-direction. The z-directed currents are mainly due to the reflector curvature and yield, for high gain antennas, minor contribution to radiated fields around the main beam. The important component which contributes to the cross-polarization is the y-component which needs to be minimized, in order to reduce the cross-polarized radiation from the reflector. This y–current component, as derived from equation (12), is given by

$$K_{vy} = \sin\theta \sin\varphi \left\{ -a_m \cos\varphi \cos(\theta/2) + a_e [\cos(\theta/2)\cos\varphi\cos\alpha - \sin\alpha \sin(\theta/2)] \right\}.$$

This cross-polarized component vanishes when both of the following conditions are satisfied:

1) $a_m = a_e$ *i.e.* equal electric and magnetic moments, and
2) $\alpha = 0$, *i.e.* the feed is pointed to the vertex of the reflector, which is the situation with symmetric center fed reflectors.

When the angle α is not zero, which is the situation with offset reflectors; especially with practical situations when the vertex is below the reflector edge, the cross-polarized current K_{vy} vanishes when both a_m and the coefficient of a_e are equal to zero. Note that the coefficient of a_m is not zero for usable offset configurations.

The condition that the coefficient of a_e be zero yields the relation

$$\tan\alpha = \cot(\theta/2)\cos\varphi.$$

From the configuration of Fig. 1 it is easy to see that this condition means lower pointing by the feed, to locations below the center of the offset reflector. When considering the locations around this center, the feed pointing is exactly at half the angle to the reflector center, *i.e.* $\alpha = \theta'/2$, where θ' is the angle to the reflector center measured from the negative z–axis. Note that when φ is different from zero in the vicinity of the reflector center, $\cos\varphi$ is reduced from unity whereas $\cot(\theta/2)$ increases by almost the same ratio keeping this condition satisfied across the reflector aperture in a plane parallel to the x-y plane. This conclusion is verified, using computer simulation, in the following section. The requirement that a_m be zero means a predominantly electric moment for the source feed.

5. Numerical Results

A computer program is written to perform the vector multiplications of equations (9) and (12), using the vector forms of the vertical polarization moments and the horizontal polarization moments. First, the simulation is performed with equal electric and magnetic moments, *i.e.* $a_e = a_m = 1$. The directivity function $f(\theta,\varphi)$ is assumed to yield reflector quadratic aperture distribution, with approximately 10 dB taper to its edge, and the feed oriented to the reflector center, at a value for $\alpha = 36°$. The reflector diameter is 3 m and its F/D (focal length to diameter ratio) is equal to unity. This reflector configuration is used for an earth station at the top of the electrical Engineering Department of King Saud University. The reflector configuration is illustrated in Fig. 2 and detailed elsewhere [5,8]. The main and cross-polarized computed current distributions are shown in Figs. 3a and 3b. It can be recognized that the depolarized currents of Fig. 3b are positive at the left side of the reflector and negative at its right side. The resulting secondary radiation pattern of the reflector is then expected to have two depolarized lobes on both sides of the main boresight beam direction. The relative level between the peak of the main polarized currents of Fig. 3a and the depolarized peak of Fig. 3b is 24 dB. Interesting is to note that the energy content of the depolarized currents is –24.24 dB relative to the main polarized currents.

5.1. Horizontally Polarized Sources

Horizontally polarized sources, with reference to Fig. 1, have the electric unit vector of polarization given by

$$\hat{a}_{ch} = \hat{a}_y ,$$

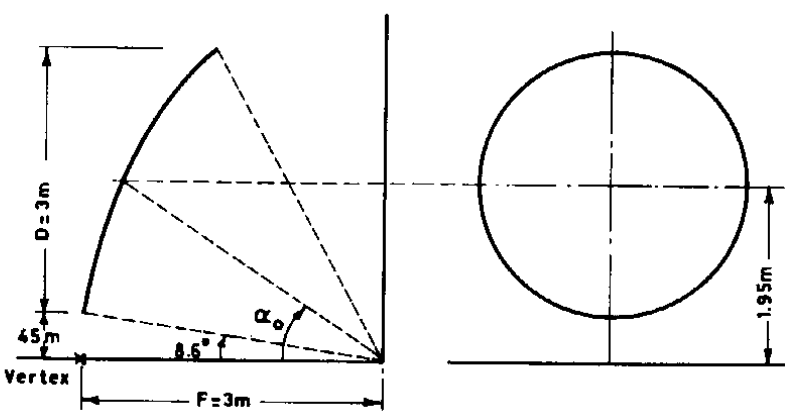

Fig. 2. The reflector configuration used in computer simulation

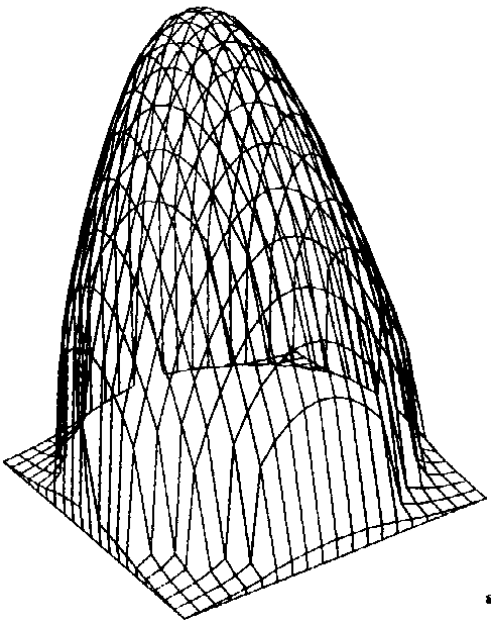

Fig. 3a. Three dimensional main polarization pattern.

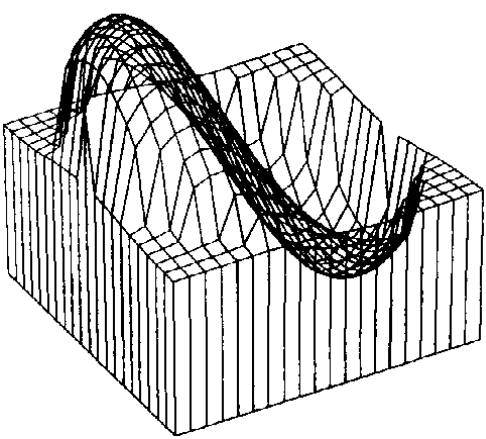

Fig. 3b. Three dimentional cross-polarization pattern.

and the magnetic unit vector of polarization given by

$$\hat{a}_{mh} = \cos\alpha\,\hat{a}_x + \sin\alpha\,\hat{a}_z$$

Substitution of these in equation (9) for the radiated magnetic fields yields an equation for $\bar{H}_{th}$ which is similar to equation (11). The magnetic field and current expressions are not detailed here as the generated computer program calculates these values for both the vertical and the horizontal polarizations. The computations for the situation when $a_m = a_e$, for horizontal polarization, with the feed oriented to the center of the reflector, are shown in the three dimensional presentations of Figs. 4a and 4b. The relative levels are exactly the same as those of Figs. 3a and 3b, *i.e.* the relative cross-polarized peak relative to the main polarization peak is also −24 db. The polarity of the cross-polarization currents, however, is reversed.

The condition for minimization of the cross-polarization currents, already examined in the situation with vertical polarization, is also tested with horizontal polarization. The same conclusions apply concerning the lower pointing of the feed to directions half way between the reflector center and its vertex. In this situation, with horizontal polarization however, the magnetic moments a_m are needed to be predominant, similar to a_e for vertical polarization. The computed cross-polarized currents are shown in Fig. 5 for the horizontal polarization and in Fig. 6 for the vertical polarization. The magnetic moments are eliminated in these figures, in order to minimize the cross-polarization for vertical polarization. Note that in these patterns the modulus is shown for better clarity of presentation. The values of the cross-polarization components are alternatively positive and negative around the center of the aperture (The feed is oriented half way between the reflector center and its vertex). The peak of the nonminimized cross-polarization component of Fig. 5 is 24 dB below the peak of the main polarization current. Note that this value is the same as the value with equal electric and magnetic moments when the feed is oriented towards the reflector center (as shown in Fig. 3). This is assumed to improve when the feed pointing is lowered, but the absence of magnetic moments in this case gave the same level as that of Fig. 3. The minimized cross-polarization for vertical polarization (using predominantly electric moment) is shown in Fig. 6. The relative level of the cross-polarization at the upper part of the reflector is −33.2 dB, while at the lower parts of the reflector these levels are at −36.5 dB.

When comparing the relative peak levels of the nonminimized currents of Fig. 5 with the energy content of these currents, as derived by integration, it is found that the latter is −24.8 dB, which is very close to the -24 dB of the former relative peaks. Also the power content of the minimized currents of Fig. 6 is −35.7 dB, compared with the relative peak levels of −33.2 dB at the upper part of the reflector and -36.5 dB at the lower part of the reflector (see Fig. 6). Since the radiation pattern is a replica of these current distributions, with factors determined by the aperture size and illumination taper, these numbers can be used for qualitative comparisons of the radiated main and cross-polarized fields, or at least for knowledge of the relative

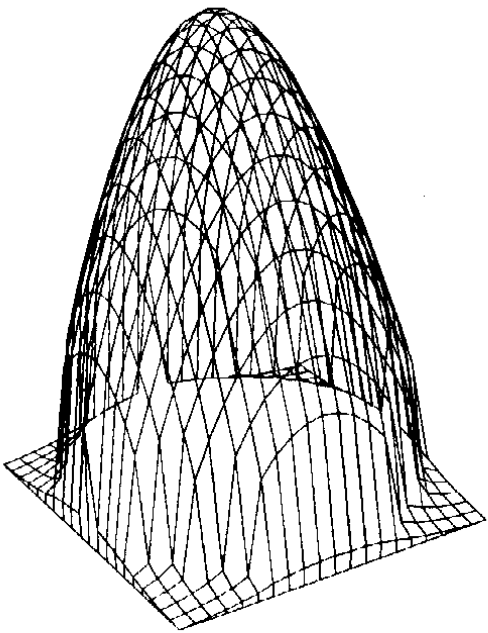

$a_m = 1$ and $a = 1$, (Horizontal Polarization)

Fig. 4a. Three dimentional main polarization pattern.

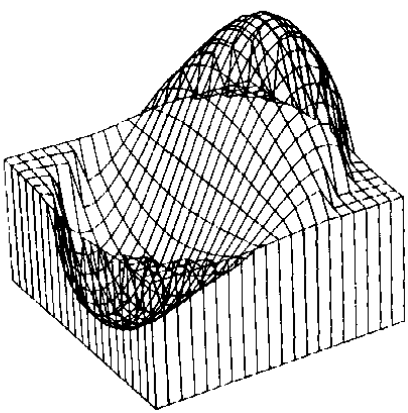

Fig. 4b. Three dimensional cross-polarization pattern.

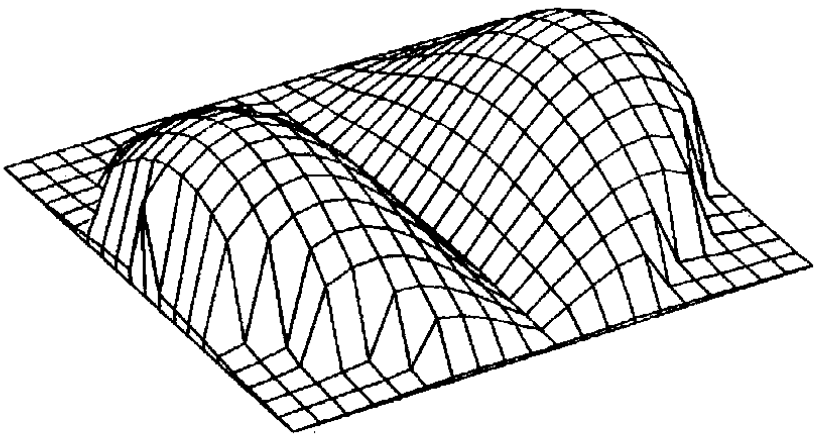

$a_e = 1$, $a_m = 0$ and $\alpha = 18°$ ($\alpha = 36°$)

Fig. 5. Non. minimized cross-polarization for horizontal polarization

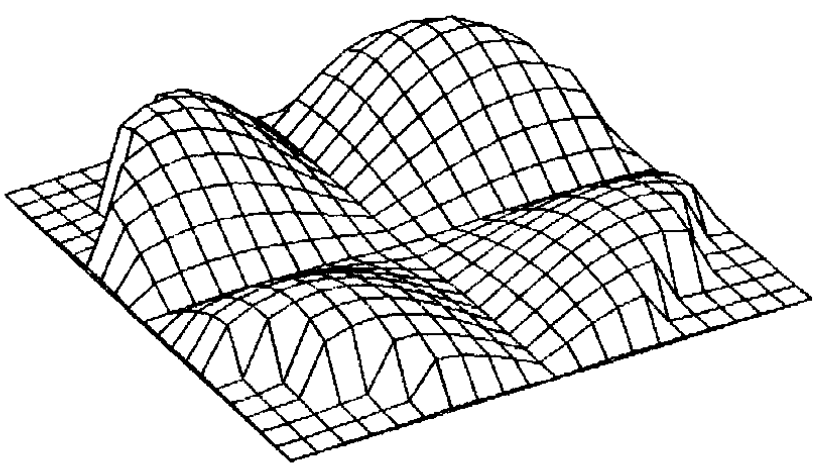

$a_e = 1$, $a_m = 0$ and $\alpha = 18°$ ($\alpha = 36°$)

Fig. 6. Minimized cross-polarization for vertical polarization

levels of radiation using different feed polarization moments. Feed designs which perform the prescribed functions in this paper are the subject of a separate study.

The minimized cross-polarization with vertical polarization needs predominantly magnetic sources. The current distributions in this situation are interchangeable with those of Figs. 5 and 6, with the exception that the positive cross-polarization for the horizontal polarization is replaced by negative cross-polarization for the vertical polarization.

6. Conclusions

Examination of our analyses indicates that minimization of the cross-polarization from offset parabolic reflectors is achievable by special feed designs having specific predominantly electric moments for vertically polarized signals (which is in this case parallel to the axis of symmetry of the reflector) or predominantly magnetic moments for horizontally polarized signals. The cross-polarization levels improvements are better than 10 dB, which brings these levels to values between −30 dB and −40 dB. These levels are high enough to allow polarization frequency reuse capabilities, doubling the channel capacity of the system. It is also important to note that improvements of the cross-polarization levels are achievable by feed pointing to directions half way between the reflector center and its vertex.

These conclusions have shown some evidence in previous practical and simulated radiation patterns performed by the author for similar antenna arrangements. The analysis of this paper form the analytical basis which are essential for feed designs and the choice of feed excitation modes which may verify the minimization requirements.

References

[1] **Afifi, M.S.** "Idealized radiators for frequency reuse applications." *IEEE, International Communications Conference (ICC) Proceedings*, (1976), pp. 4-15/20, Philadelphia, Pa, U.S.A.

[2] **Afifi, M.S.; Thomas, R. and Meier, R.** "Depolarized radiated fields and currents of reflector antennas." *IEEE AP-S Symposium*, June (1977), San Francisco, Ca, U.S.A.

[3] **Silver, S.** *Microwave Antenna Theory and Design*. Rad. Lab. Series, 12, New York: McGraw Hill, 1949.

[4] **Afifi, M.S.** "Scattered radiation from microwave antennas and the design of the paraboloid-plane reflector antenna." *D. Sc. Thesis*, Delft University of Technology, Holland, (1967).

[5] **Nagi, M.; Afifi, M.S. and Samarkandy, M.K.** "Feed design and performance of an offset reflector of a small earth station." *Arabsat Symposium Proceedings*, 29 Sep. - 1 Oct. (1987), pp. 395-406, Riyadh, Saudi Arabia.

[6] **Stratton, J.A.** *Electromagnetic Theory*, Sect. 1.11. New York: Mc.Graw-Hill Book Company, 1941.

[7] **Balanis, C.A.** *Antenna Theory, Analysis and Design*, pp. 83, 604-646. N.Y.: Harper & Row, Publishers, 1982.

[8] **Afifi, M.S. and Samarkandy, M.K.** "The limitations and the future of small earth stations." *5th World Telecommunication Forum Proceedings*, ITU TELECOM'87, Part 2, (1987), pp. 203-207, Geneva, Switzerland.

(*Manuscript Received:* 6-12-1987; *Accepted:* 27-2-1988)

تحليل وضبط تيارات الاستقطاب المتعامدة للهوائيات العاكسة مكافئة القطع

مصطفى سيد عفيفي

قسم الهندسة الكهربائية، كلية الهندسة، جامعة الملك سعود، ص.ب ٨٠٠، الرياض ١١٤٢١، المملكة العربية السعودية

ملخص البحث: يقدم هذا البحث تحليلاً لتوزيع كثافة التيارات على أسطح الأجزاء المختلفة من الهوائيات العاكسة مكافئة المقطع باستخدام مغذي في صورة عامة وتوجيهًا محدودًا في اتجاه السطح العاكس. وتحدد هذه التحليلات الرياضية الخلط اللازم بين المكونات الكهربية والمغناطيسية الأساسية للمغذي والتي تتحكم في تقليل كثافة التيارات المتعامدة. وتعتمد هذه النسبة على شكل السطح العاكس واستقطاب الموجات. ففي حين أنه من المعروف انعدام التيارات المتعامدة في حالة تناسق السطح العاكس حول محوره مع تساوي الخلط الكهربي والمغناطيسي للمغذي فإن التحليلات الخاصة بالأسطح المائلة الناقصة غير متواجدة. ولقد نتج عن هذا البحث معادلات شاملة لتحديد هذه التيارات المتعامدة بصفة عامة وللهوائيات المائلة الناقصة بصفة خاصة، نظرًا لاتساع نطاق استخداماتها في الاتصالات الحديثة.

تتلخص النتائج في أن التيارات المتعامدة يمكن فقط تقليلها للهوائيات الناقصة المائلة. وذلك بتوجيه المغذي لنقاط أسفل اتجاه مركز السطح العاكس وبالتحديد في منتصف المسافة بين المركز ومحور السطح. كذلك فإن المغذي يجب أن يكون ذا عزم كهربائي عند استخدام الاستقطاب الرأسي (الموازي لخط تماثل العاكس) ويجب أن يكون ذا عزم مغناطيسي عند استخدام الاستقطاب الأفقي. كما يعرض هذا البحث توضيحًا كميًا لهذه الحقائق باستخدام برامج أعدت خصيصًا على الحاسب الآلي.